Lasers in Manufacturing Conference 2023

Fs-laser fabrication of PMN-PT piezo actuators

Sandra Stroj[a,*], Barbara Lehner[b], Julia Freund[b,c], Armando Rastelli[b], Fadi Dohnal[a]

[a] *Research Center for Mikrotechnology, FH Vorarlberg, Hochschulstraße 1, A-6850 Dornbirn, Austria*
[b] *Institute of Semiconductor and Solid State Physics, Johannes Kepler University, Altenbergerstraße 69, A-4040 Linz, Austria*
[c] *Institut für Theoretische Physik, Universität Innsbruck, Technikerstraße 21a, 6020 Innsbruck, Austria*

Abstract

Due to its outstanding piezoelectrical properties, single-crystal PMN-PT has proven to be a very promising material for actuator applications. However, PMN-PT is very difficult to process by conventional technological methods since it is very sensitive to thermal and mechanical load. In this work we demonstrate that surface structuring as well as high aspect-ratio cutting is possible using a femtosecond laser. We realised a laser generated actuator platform for tuning the optical emission of an entangled photon source by introducing biaxial strain. The strain-tuning device with a size of 5x5 mm² is realized in a two-step laser process where the electrical contacts for individual control of six actuator legs are structured by selective laser removal of a thin gold layer, followed by the PMN-PT structuring and cutting process. This method is to our knowledge unique for realizing complex and miniaturized actuators based on single crystal piezoelectrical materials.

Keywords: femtosecond laser, cutting, actuator, strain-tuning

1. Introduction

In the field of novel actuators, single-crystal PMN-PT has proven to be a very promising piezoelectric material. However, the possibility of using this material with high innovation potential depends essentially on the extent to which it can be processed with the necessary precision and quality. Previous approaches are chemical etching (Peng et al., 2008), reactive ion etching (Zhang et al., 2015), UV laser ablation (Ivan et al., 2012; Lam et al., 2013) or ion milling (Chen et al., 2017). With the chosen method, the crystalline quality of the substrate must be preserved as much as possible during processing. Furthermore, the weakening of the strength through the introduction of cracks must be minimised as far as possible. The mentioned

* Corresponding author. Tel.: +43-5572-792-7207; fax: +43-5572-7207-9501.
E-mail address: sandra.stroj@fhv.at.

methods have disadvantages like the long processing time, the introduction of too much damage to the substrate material or the limited flexibility.

We show in this work that processing with the fs-laser is a promising method for the creation of complex and miniaturized actuators based on PMN-PT single crystals. It allows the realisation of arbitrary geometries with minimal mechanical as well as thermal stress. In addition, the non-thermal ablation process does not affect the crystalline structure near the processed edges, which allows the realisation of actuators without limiting the material performance. An additional advantage of processing with the femtosecond laser is the mask-free processing in the micrometre range. Since the substrates are usually not in wafer form, the implementation of standard technology processes is more difficult. We demonstrate the realization of a six-leg piezo actuator based on PMN-PT, a configuration used for biaxial strain-tuning of quantum dot entangled photon emitters (Lehner et al., 2023; Lettner et al., 2021; Martín-Sánchez et al., 2018; Martín-Sánchez et al., 2016; Rota et al., 2022).

2. Material and Methods

For this work single crystal PMN0.71 − PT0.29 (TRS crystals) with a thickness of 500 µm and a size of 10x10 mm² was used. The piezo substrates were lapped down to the thickness of 300 µm and mechanically polished. Subsequent physical vapor deposition of thin metallic layers (10 nm Ti/100 nm Au) on both sides forms the electrical contacts of the piezo actuator.

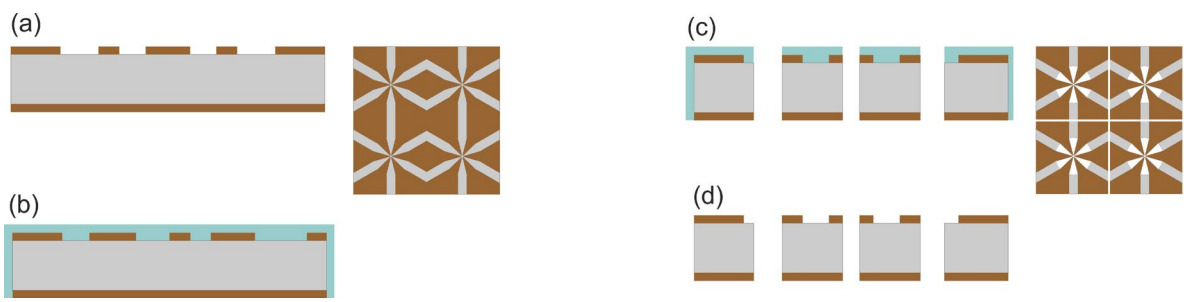

Fig. 1. Process chain for the fabrication of a piezo actuator device using femtosecond-laser structuring and cutting.

The process chain for the laser fabrication of the piezo actuators is shown schematical in Fig. 1. In a first step, the gold layer is patterned by selective laser structuring (see Fig. 1 (a)). This allows the actuator leg contacts to be created. As a next step the piezo substrate is covered with a thick layer of PVA (poly vinyl alcohol) (see Fig.1 (b)). Following this, the actuator legs are generated by laser cutting (see Fig.1 (c)). In the same process step the substrate is separated into four identical actuator chips. The debris, deposited in the vicinity of the cutting paths, is then removed by a washing step where the water solvable PVA layer is removed. This allows a complete fabrication of four actuator chips with a fast and flexible process and is advantageous for further integration to realise a complete platform.

For the selective structuring step as well as the cutting task we used a femtosecond laser (Spirit®, Spectra-Physics) with a pulse duration of 380 fs and a pulse repetition rate of up to 1 MHz. For the selective structuring of the gold layer the laser was operated at a repetition rate of 1 MHz which was reduced to a frequency of 100 kHz by means of an acousto-optic modulator. In this laser operation regime, the low pulse energy levels

required for selective ablation of thin metal films can be set with the needed accuracy. Higher values of pulse energy are necessary for cutting the actuators. For this reason, the repetition rate was set to a value of 200 kHz where the laser offers its maximum pulse energy. Due to the high thermal sensitivity of the material and the tendency to form cracks and chippings, it was necessary to reduce the frequency to 25 kHz by using the acousto-optic modulator.

The laser was operated at its second harmonic with a wavelength of 520 nm and was focused by a 170 mm f-theta objective onto the sample surface to a spot with a 21 µm diameter.

3. Results and Discussion

3.1. Selective ablation of thin metal layer

Due to the temporal decoupling of energy input and material removal, machining with ultrashort laser pulses shows precisely defined values of the ablation threshold. A well established procedure for determining the ablation threshold as well as the beam diameter when using lasers with Gaussian beam profiles is Liu's method (Liu, 1982) .

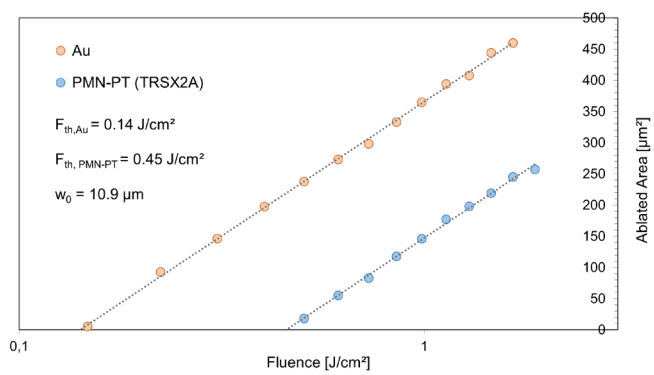

Fig. 2. Liu plot of the single pulse ablation thresholds φ of gold as well as PMN-PT. The gold layer shows a significantly lower ablation threshold compared to PMN-PT enabling selective gold removal.

In this method, one plots the ablated circular area generated by laser pulses versus the logarithm of the pulse fluence; from these plots, one obtains both beam radius and ablation threshold with a linear fit. Liu plots for single-pulse ablation of PMN-PT and the gold layer are shown in Fig. 2; the measured value of the ablation threshold for PMN-PT is 0.45 J cm^{-2} and for gold is 0.14 J cm^{-2}. This offers a process window for structuring the gold layer without any material removal of the underlying substrate.

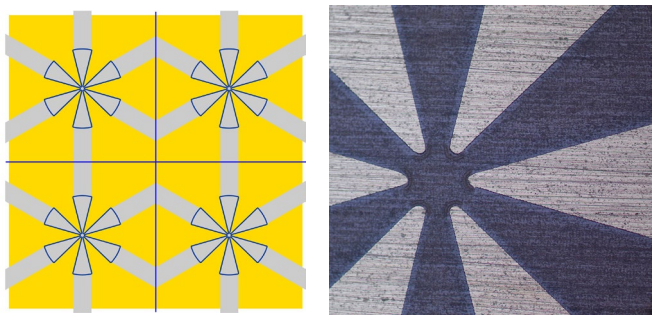

Fig. 3. The schematic image shows the design of the piezo actuator. The yellow part represents the substrate with the gold layer and the grey part is the area where the metal layer will be removed to form the electrical contacts. The blue lines show the cutting paths for the subsequent laser cutting of the final piezo actuators and the chip separation. The microscope image on the right shows the central part of the actuator after removing of the gold layer.

For the thin film removal, the contact geometry (grey area in Fig. 3 left) was filled with a line pattern with a pulse spacing of 5 micrometres. The pulse repetition rate was 100 kHz and the pulse energy was set to 0.8 µJ. The fluence used for layer removal is with a value of 0.13 J cm^{-2} outside the previously determined process window. This can be explained by the fact that the ablation thresholds are determined for single pulses. However, the ablation threshold decreases when machining with multiple pulses due to accumulation effects. This is the case with a pulse overlap of 75% as in our case. After two repetitions of the hatch pattern, the gold layer was completely removed as can be seen in the optical microscope image of Fig. 3 on the right.

3.2. Piezo cutting

We perform experiments with laser polarization perpendicular and parallel to the direction of the cut (and therefore respectively p and s with respect to the cut walls) as well as with circular polarized light.

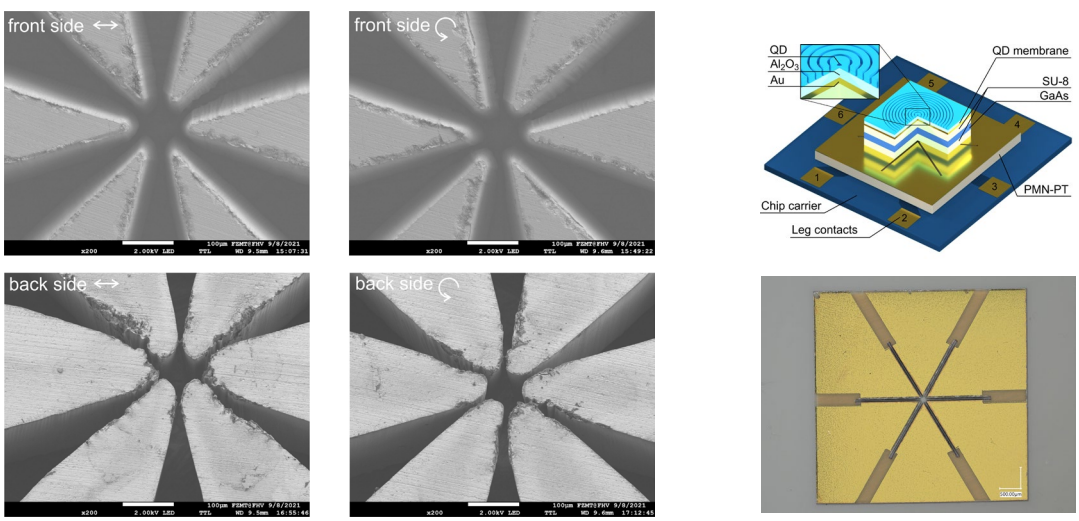

Fig. 4. SEM images of the central part of the actuator after the cutting with linear (images on the left) and circular polarized (images second column) light. The upper row shows the laser entrance side, the pictures below the laser exit side. The optical microscope image on the right shows the final actuator (design variation) as it is integrated into the strain tuning device shown in the schematic drawing above (Rota et al., 2022).

Cracks are formed at the edge of the cuts in the case of p-polarized laser light starting from about the fluence of 2.2 J cm^{-2} , while s-polarized light does not cause cracks up to our maximum fluence of 3.1 J cm^{-2}. The different crack formation between s- and p-polarized light can be due to a higher absorption of p-polarized light at the inclined walls.

For the given actuator geometry, the polarization cannot be chosen as the devices have complex contours that lead to a position-dependent polarization. In addition, the different side-wall coupling of the laser polarization results in a slightly distorted geometry at the laser exit side (see SEM images in Fig. 4). For this reason, experiments were done using circular polarized light. Given these observations, for the fabrication of the final devices we select the following set of parameters: 2.2 J cm^{-2} fluence, 25 kHz repetition rate, 5 µm pulse spacing and circular polarized light. At this fluence value the wall angle is approximately of 85°; since we perform our fabrication on 300 µm-thick crystals, we need to place 10-15 parallel laser cuts to cut through the crystal consistently. With a cutting pattern repetition of up to 400, guaranteed cutting through with high edge definition on the laser exit side is ensured. The laser focus is positioned 100 µm below the sample surface. Since the substrate thickness is far below the Rayleigh length of 600 µm, changing the focus position during cutting was not necessary.

References

Chen, Y., Zhang, Y., Keil, R., Zopf, M., Ding, F., Schmidt, O.G., 2017. Temperature-Dependent Coercive Field Measured by a Quantum Dot Strain Gauge. Nano Lett. 17, 7864–7868. https://doi.org/10.1021/acs.nanolett.7b04138

Ivan, I.A., Agnus, J., Lambert, P., 2012. PMN–PT (lead magnesium niobate–lead titanate) piezoelectric material micromachining by excimer laser ablation and dry etching (DRIE). Sens. Actuators Phys. 177, 37–47. https://doi.org/10.1016/j.sna.2011.09.015

Lam, K.H., Chen, Y., Au, K., Chen, J., Dai, J.Y., Luo, H.S., 2013. Kerf profile and piezoresponse study of the laser micro-machined PMN-PT single crystal using 355nm Nd:YAG. Mater. Res. Bull. 48, 3420–3423. https://doi.org/10.1016/j.materresbull.2013.05.025

Lehner, B.U., Seidelmann, T., Undeutsch, G., Schimpf, C., Manna, S., Gawełczyk, M., da Silva, S.F.C., Yuan, X., Stroj, S., Reiter, D.E., Axt, V.M., Rastelli, A., 2023. Beyond the four-level model: Dark and hot states in quantum dots degrade photonic entanglement. Nano Lett. 23, 1409–1415. https://doi.org/10.1021/acs.nanolett.2c04734

Lettner, T., Gyger, S., Zeuner, K.D., Schweickert, L., Steinhauer, S., Reuterskiöld Hedlund, C., Stroj, S., Rastelli, A., Hammar, M., Trotta, R., Jöns, K.D., Zwiller, V., 2021. Strain-Controlled Quantum Dot Fine Structure for Entangled Photon Generation at 1550 nm. Nano Lett. 21, 10501–10506. https://doi.org/10.1021/acs.nanolett.1c04024

Liu, J.M., 1982. Simple technique for measurements of pulsed Gaussian-beam spot sizes. Opt. Lett. 7, 196. https://doi.org/10.1364/OL.7.000196

Martín-Sánchez, J., Trotta, R., Mariscal, A., Serna, R., Piredda, G., Stroj, S., Edlinger, J., Schimpf, C., Aberl, J., Lettner, T., Wildmann, J., Huang, H., Yuan, X., Ziss, D., Stangl, J., Rastelli, A., 2018. Strain-tuning of the optical properties of semiconductor nanomaterials by integration onto piezoelectric actuators. Semicond. Sci. Technol. 33, 013001. https://doi.org/10.1088/1361-6641/aa9b53

Martín-Sánchez, J., Trotta, R., Piredda, G., Schimpf, C., Trevisi, G., Seravalli, L., Frigeri, P., Stroj, S., Lettner, T., Reindl, M., Wildmann, J.S., Edlinger, J., Rastelli, A., 2016. Reversible Control of In-Plane Elastic Stress Tensor in Nanomembranes. Adv. Opt. Mater. 4, 682–687. https://doi.org/10.1002/adom.201500779

Peng, J., Chao, C., Dai, J., Chan, H.L.W., Luo, H., 2008. Micro-patterning of 0.70Pb(Mg1/3Nb2/3)O3–0.30PbTiO3 single crystals by ultrasonic wet chemical etching. Mater. Lett. 62, 3127–3130. https://doi.org/10.1016/j.matlet.2008.02.003

Rota, M.B., Krieger, T.M., Buchinger, Q., Beccaceci, M., Neuwirth, J., Huet, H., Horová, N., Lovicu, G., Ronco, G., da Silva, S.F.C., Pettinari, G., Moczała-Dusanowska, M., Kohlberger, C., Manna, S., Stroj, S., Freund, J., Yuan, X., Schneider, C., Ježek, M., Höfling, S., Basset, F.B., Huber-Loyola, T., Rastelli, A., Trotta, R., 2022. A source of entangled photons based on a cavity-enhanced and strain-tuned GaAs quantum dot (No. arXiv:2212.12506). arXiv.

Zhang, J., Ren, W., Jing, X., Shi, P., Wu, X., 2015. Deep reactive ion etching of PZT ceramics and PMN-PT single crystals for high frequency ultrasound transducers. Ceram. Int. 41, S656–S661. https://doi.org/10.1016/j.ceramint.2015.03.258